Medical Image Denoising using Adaptive Spatial Domain Schemes with Additive Noise

Osama Qasim Jumah Al-Thahab
University of Babylon, Department of Electric
eng.osama.qasim@uobabylon.edu.iq
Hanaa mohsin ali
University of Babylon, Department of Electric
ahanaamohsin@yahoo.com.

Abstract

Image denoising is one of the most significant tasks in medical image processing due to the significant information obtained by these images related to the human body or the tissues of the body's organs. So, many methods have been proposed for removing the noise that affects the medical images. In this research a new algorithm has been proposed for denoisning medical images work in spatial domain. A new algorithm depends on the idea that combine between characteristic of different filters which work in spatial domain with adaptive sizes of windows for reaching to the acceptance results in remove noise from medical images. This algorithm called Adaptive Window Wiener Filter (AWWF). Two types of medical images and noise that corrupt these medical image used in this research. The first type is Poisson noise which corrupts X-ray medical images and the second type is Rician noise which corrupts MRI medical images. The algorithm begins with using a median filter on a noisy image to get the blurred version of the image. Then using an edge detection algorithm, the edges detection of the resulted blurred image is found by using the Prewitt operator. Then Wiener filter of variable size windows is applied throughout the noisy image to suppress the noise. The window size is made bigger in homogenous and smooth regions and is made smaller in edge and complex regions.
Keywords: Image processing, Image Denoising, Additive noise.

الخلاصة

تعد عملية إزالة الضوضاء من الصور من ابرز المهام في مجال معالجة الصور الطبية بسبب المعلومات المهمة المستخلصة من هذه الصور والتي تخص الجسم البشري أو أنسجة أعضاء الجسم .لهذا السبب فقد اقترحت عدة طرق لإزالة الضوضاء من الصور الطبية . في هذا البحث اقترحت طريقه جديدة لإزالة الضوضاء من الصور الطبية التي تعمل في المجال ألحيزي. الخوارزمية الجديدة تعتمد على فكرة الجمع بين خصائص المرشحات المختلفة التي تعمل في المجال ألحيزي مع تنويع أحجام النوافذ للوصول الى النتائج المطلوبة في إزالة الضوضاء من الصور الطبية. هذه الطريقة تدعى خوارزمية النافذة المحدثة لمرشح wiener. استخدم في هذا البحث نوعان من الصور الطبية والضوضاء التي تصيب هذه الصور. النوع الأول من الضوضاء هو ضوضاء Poisson التي تصيب صور الأشعة السينية الطبية والنوع الثاني هو ضوضاء Rician التي تصيب صور MRI الطبية. الخوارزمية تبدأ باستخدام المرشح الوسيط على الصور المشوشة للحصول على نسخة ضبابية من الصورة .بعدها نستخدم خوارزمية تحديد الحافات .تحديد الحافات للصورة الضبابية الناتجة أوجد باستخدام معامل Prewitt. ثم يتم تطبيق مرشح wiener مع نوافذ بأحجام مختلفة على الصورة المشوشة للتخلص من التشويش. حجم النافذة يكون كبير في المناطق الناعمة والمتشابهة ويكون اصغر في مناطق الحافة والمعقدة.
الكلمات المفتاحية:– معالجة الصور, تحليل الصور, الضوضاء المضافة.

1. Introduction

The field of digital image processing refers to processing digital images by means of a digital computer. A digital image can be considered as a discrete representation of data possessing both spatial (layout) and intensity (color) information. It is composed of a finite number of elements, each of which has a particular location and value. These elements are called picture elements, image elements, pels, and pixels. Pixel is the term used most widely to denote the elements of a digital image. Digital image processing techniques began in the late 1960s and early 1970s to be used in medical imaging, remote Earth resources observations, and astronomy. Medical imaging has been undergoing a revolution in the past decade with the advent of faster,

more accurate, and less invasive devices. This has driven the need for corresponding software development, which in turn has provided a major impetus for new algorithms in signal and image processing. Medical images typically suffer from one or more of the following imperfections:

a) Low resolution (in the spatial and spectral domains).
b) High level of noise.
c) Low contrast.
d) Geometric deformations.
e) Presence of imaging artifacts.

These imperfections can be inherent to the imaging modality (e.g., X-rays offer low contrast for soft tissues, ultrasound produces very noisy images, and metallic implants will cause imaging artifacts in Magnetic Resonance Imaging MRI) or the result of a deliberate trade-off during acquisition. Several tasks can be performed semi-automatically to support the eye brain system of medical practitioners. Smoothing is the problem of simplifying the image while retaining important information. Registration is the problem of fusing images of the same region acquired from different modalities or putting in correspondence images of one patient at different times or of different patients. Finally, segmentation is the problem of isolating anatomical structures for quantitative shape analysis or visualization. The ideal clinical application should be fast, robust with regards to image imperfections, simple to use, and as automatic as possible. The ultimate goal of artificial vision is to imitate human vision, which is intrinsically subjective (Rashid Ismael 2011)

Digital images can be corrupted by noise during the process of acquisition and transmission, degrading their quality. A major challenge is to remove as much as possible of the noise without eliminating the most representative characteristics of the image, such as edges, corners and other sharp structures. Several approaches have been proposed to suppress the presence of noise in digital images, many of them based on spatial filters. These filters usually smooth the data to reduce noise effects; however, this process can cause image blurring or edge removal (Zhang, 2009). Many techniques for improving spatial filters have been developed by removing the noise more effectively while preserving edges in the data. Some of these techniques are based on partial differential equations and computational fluid dynamics such as level set methods, total variation (TV) methods, non-linear isotropic and anisotropic diffusion, and essentially non-oscillatory schemes (Rodrigo and Pedrini 2012).

2. Noise in Medical Image

Noise will be inevitably introduced in the image acquisition process and de-noising is an essential step to improve the image quality. As a primary low-level image processing procedure ,noise removal has been extensively studied and many de-noising schemes have been proposed, from the earlier smoothing filters and frequency domain de-noising methods to the lately developed wavelet, curvelet and ridge let based methods, sparse representation and K-SVD methods, shape-adaptive transform, bilateral filtering, non-local mean based methods and non-local collaborative filtering. With the rapid development of modern digital imaging devices and their increasingly wide applications in our daily life, there are increasing requirements of new de noising algorithms for higher image quality (Zhang 2009).

Digital images may be contaminated by different sources of noise. Noise may be generated due to imperfect instruments used in image processing, problems with the data acquisition process, and interference, all of which can degrade the data of interest. Furthermore, noise can be introduced by transmission errors and compression also. Different types of noises are introduced by different noise sources like dark

current noise is due to the thermally generated electrons at sensor sites. It is proportional to the exposure time and highly dependent on the sensor temperature. Shot noise, which has the characteristics of Poisson distribution, is due to the quantum uncertainty in photoelectron generation. Amplifier noise and quantization noise occur during the conversion of number of electrons to pixel intensities. The overall noise characteristic in an image depends on many factors, which include sensor type, pixel dimensions, temperature, exposure time, and ISO speed.

Noise is also channel dependent. Typically, green channel is the least noisy while blue channel is the noisiest channel. That means noise is in general not white. Noise in a digital image has low as well as high frequency components. Though the high-frequency components can easily be removed, it is challenging to eliminate low frequency noise as it is difficult to distinguish between real signal and low-frequency noise. Most of the natural images are assumed to have additive random noise, which is modeled as Gaussian type. Speckle noise is observed in ultrasound images, whereas Rician noise affects MRI images. Thus, denoising is often a necessary and the first step to be considered before the image data is analyzed. It is necessary to apply an efficient denoising technique to compensate for any data corruption. The goal of denoising is to remove the noise while preserving the important image information as much as possible (Roy *et al.*, 2010).

3. Medical Imaging Technology

Medical imaging systems detect different physical signals arising from a patient and produce images. An imaging modality is an imaging system which uses a particular technique. Some of these modalities use ionizing radiation with sufficient energy to ionize atoms and molecules within the body, and others use non-ionizing radiation . Appendix A contains test images of these modalities which include:

3.1. X-ray Radiography

X-rays are among the oldest sources of Electromagnetic radiation used for imaging. The best known use of X-rays is medical diagnostics, but they also are used extensively in industry and other areas, like astronomy (Gonzalez *et al.*, 2002). In projection or planar X-ray radiography the image is a simple two dimensional projection or shadow gram of a three-dimensional object, the part of the patient in the field of view; X-ray film is the detector. Projection radiography includes (Dougherty, 2009):

- Film-screen radiography, including chest radiography, abdominal radiography, angiography (studies of blood vessels) and mammography.
- Fluoroscopy, in which images are produced in real time using an image intensifier tube to detect the X-rays.
- Computed radiography, in which a re-usable imaging plate containing storage phosphors replaces the film as the detector.
- Digital radiography, which uses semiconductor sensors.

3.2. Magnetic Resonance Imaging

Magnetic resonance imaging (MRI) is a non-ionizing technique that uses radio frequency (200 MHz–2 GHz) electromagnetic radiation and large magnetic fields (around 1–2 tesla, compared with the Earth's magnetic field of about $0.5 \times 10{-}4$ tesla) (Dougherty, 2009). This technique relies on the relaxation properties of magnetically excited hydrogen nuclei of water molecules in the body. Images are created from the difference in relaxation rates in different tissues (Angenent *et al.*, 2006). It has several advantages over other imaging techniques enabling it to provide

three-dimensional (3-D) data with high contrast between soft tissues (Zhang *et al.*, 2001).

4. Medical image denoising

Image denoising is a procedure in digital image processing aiming at the removal of noise, which may corrupt an image during its acquisition or transmission, while retaining its quality. Medical images obtained from MRI are the most common tool for diagnosis in Medical field. These images are often affected by random noise arising in the image acquisition process. The presence of noise not only produces undesirable visual quality but also lowers the visibility of low contrast objects. Noise removal is essential in medical imaging applications in order to enhance and recover fine details that may be hidden in the data (Satheesh1 *et al.*, 2011). Linear filtering techniques, such as Wiener filter or match filter, have been used for this purpose for many years. But linear filters may result in some problems, such as blurring the sharp edges, destroying lines and other finer image details. They generally fail to effectively remove heavy tailed noise. Due to these facts, an alternative filtering technique like nonlinear filtering is necessary. Many works have been reported on image denoising using nonlinear filters. Thresholding algorithm in an orthogonal transform domain, such as subband or wavelet transform, is a nonlinear filter. Sub band transform with orthogonal perfect reconstruction filter-banks is an orthogonal transform. It is known that the sub-band filters act as a set of discrete time based functions in a vector space and the decomposition of signal is just to project the signal onto these base functions. As for a signal with noise, there are some differences between the coefficients of original signal and noise because of their different features (Roy *et al.*, 2010).

5. Noise Models in Medical Images

Medical images are generally of poor contrast and get complex types of noise due to various acquisitions, transmission, storage and display devices, and also because of application of different types of quantization, reconstruction and enhancement algorithms (Rashid Ismael, 2011). A common misconception in image processing is to assume noise to be additive with a zero-mean, constant-variance Gaussian distribution or to be Poisson distributed. This assumption simplifies image filtering and deblurring, but the poor quality of the results generally indicates that a better understanding of the noise properties is required. The noise on MRI images was found to have a Rician probability density function instead of a Gaussian one whereas the noise on computed Satheesh1 *et al.*, 2011). The main disadvantage of medical ultrasonography is the poor quality of images, which are affected by multiplicative speckle noise (Rashid Ismael, 2011). Then the common types of noise found in medical imaging are (Gravel *et al.*, 2004):

5.1 Gaussian Noise

Gaussian noise takes the bell-shaped curve distribution, which can analytically be described as (Abdulmunim, 2004):

$$P(x) = \frac{1}{\sqrt{2\pi\sigma^2}} \ell^{-(x-\mu)^2} / 2\sigma^2 \quad \text{……………………………………….. (1)}$$

Where (x) is the gray level, (μ) is the mean and (σ) is the standard deviation and (σ^2 is the variance).Approximately 70% of its pixel values are in the range [(x − μ), (x + μ)]. Gaussian noise comes from many natural sources, such as the thermal vibrations of atoms in antennas (referred to as thermal noise or Johnson noise) and black body radiation from warm objects (Dougherty, 2009).

5.2 Poisson Noise

Photon noise results from the statistical nature of electromagnetic waves, which include visible light, X-rays and γ-rays: all are emitted as packets of energy, photons, with a probability distribution that is a Poisson distribution (Dougherty, 2009). Typical examples are found in standard X-ray films, Charge-Coupled Device cameras, and infrared photometers (Gravel *et al.,* 2004).

5.3 Rician Noise

MRI image has two images (X_1 and X_2) acquired in quadrature. Each image is degraded by a zero-mean Gaussian noise of standard deviation (σ) (which is defined as the noise level). The two images are then combined into a magnitude image (X) and the Gaussian noise pdf is transformed into a Rician noise pdf described by:

$$P(x) = \frac{1}{\sigma^2} \ell^{(\frac{X^2+S^2}{2\sigma^2})} I_0 \quad (\frac{X.S}{\sigma^2}) \quad \ldots\ldots\ldots\ldots\ldots\ldots\ldots\ldots\ldots\ldots\ldots\ldots\ldots\ldots\ldots\ldots\ldots\ldots (2)$$

Where (I) is the modified Bessel function of the first kind with order zero, (S) is the image pixel intensity in the absence of noise, and (X) is the measured pixel intensity. When S σ (high SNR) equation (2.5) is described as:

$$P(X) \approx \frac{1}{\sqrt{2\mu\sigma^2}} \ell^{-\frac{(X^2-\sqrt{S^2+\sigma^2}^{\,2})^2}{2\sigma^2})} \approx \frac{1}{\sqrt{2\mu\sigma^2}} \ell^{\frac{-(X^2-S)^2}{2\sigma^2}} \quad \ldots\ldots\ldots (3)$$

This equation shows that for image regions with high intensities the noisy data distribution can be considered as a Gaussian distribution with variance (σ^2) and mean ($\mu = S$). A special case of the Rician distribution in image regions where only noise is present (S = 0) is known as the Rayleigh distribution and is described by:

$$P(X) = \frac{X}{\sigma^2} \ell^{\frac{-X^2}{2\sigma^2}} \quad \ldots\ldots\ldots\ldots\ldots\ldots\ldots\ldots\ldots\ldots\ldots\ldots\ldots\ldots\ldots\ldots\ldots\ldots\ldots\ldots\ldots\ldots\ldots\ldots (4)$$

Rician noise differs greatly from Gaussian and Poisson noises. The variance of a Gaussian noise is constant whereas the variance of a Poisson noise is proportional to the noise mean. Rician noise is such that the noise variance depends non-linearly on the noise mean (Rashid Ismael, 2011).

6. Medical image denoising using filtering

Mean and Wiener filters suppress additive white Gaussian noise from an image very effectively under low and moderate noise conditions. But, these distort and blur the edges unnecessarily. Lee filter and non-local means (NL-Means) filter work well under very low noise condition. The *method noise* (Buades *et al.,* 2005) for these filters is low as compared to other spatial-domain filters. The computational complexity of simple mean filter is low whereas that of NL-Means filter is very high. Mean, Wiener, Lee and NL-means filters are incapable of suppressing the Gaussian noise quite efficiently under high noise conditions. Therefore, some efficient spatial-domain filters should be designed with the following ideal characteristics.

i) Suppressing Gaussian noise very well under low, moderate and high noise conditions without distorting the edges and intricate details of an image;
ii) Having low *method noise*; and
iii) Having less computational complexity.

In this research, spatial-domain image denoising schemes is proposed. The Adaptive Window Wiener filter (AWWF) developed here is a very good scheme to suppress Rician` and Poisson noises under moderate noise conditions. In this work used the median and wiener filter to improve filter behavior with high noise conditions.

7. Development of Adaptive Window Wiener Filter

An Adaptive Window Wiener Filter (AWWF) is developed for suppressing Gaussian noise under low *(the noise standard deviation, $\sigma_n \leq 10$)* and moderate noise *($10 < \sigma_n \leq 30$)* conditions very efficiently. But, it does not perform well under high noise *($30 < \sigma_n \leq 50$)* conditions. This filter is a modified version of Wiener filter (I. H. Jang and N. C. Kim 1997) where the size of the window varies with the level of complexity of a particular region in an image and the noise power as well. A smooth or flat region (also called as homogenous region) is said to be less complex as compared to an edge region. The region containing edges and textures are treated as highly complex regions. The window size is increased for a smoother region and also for an image with high noise power. Since the edges in an image are specially taken care of in this algorithm, the proposed filter is found to be good in edge preservation.

The work begins by using a mean filter on a noisy image to get the blurred version of the image. Using the edge extraction operator, the edges of the resulted blurred image is found out. The Wiener filter of variable size is applied throughout the noisy image to suppress the noise. The window size is made larger in smooth regions and is kept smaller in the regions where edges are located. This scheme is adopted not to blur a complex or edge region too much. It is a fact that a noise-free sample can be estimated with better accuracy from a large number of noisy samples. Similarly, in order to estimate a true pixel in a particular region from a noisy 2-D image, a large number of pixels in the neighborhood surrounding the noisy pixel are required. In other words, a larger-sized window, surrounding the pixel to be filtered, can be considered for better estimation.

In a homogenous region, the correlation amongst the pixels is high. Hence, a larger sized window can be taken if the pixel to be filtered belongs to a homogenous region. On the other hand, a pixel that belongs to a non-homogenous region or the region containing edges has got less number of correlated pixels in its neighborhood. In such a case, smaller-sized window has to be taken for denoising a pixel belonging to a non-homogenous region. However, a little bit of noise will still remain in the non homogenous or edge region even after filtration. But human eye is not so sensitive to noise in any edge region. Hence, a variable sized window may be a right choice for efficient image denoising. In the proposed adaptive window Wiener filter, the window is made adaptive i.e. the size of the window varies from region to region. In a flat or homogenous region, the size of the window taken is large enough. The size of window is small in the regions containing edges. The problem here is to distinguish the edge and smooth regions. The edges and smooth regions are easily distinguished if the edge extraction operators are used. Many edge extraction operators such as Sobel, Canny, Roberts, Prewitt etc. are proposed in the literature (Chaira, and Ray, 2008), But, finding the true edges in a noisy environment is not so easy.

The edge extraction operator works well on noise free images. So, it is important to make the noisy image a little bit blurred before edge extraction. In the proposed filter, the mean filter of window size 5×5 is used when the noise level is low and moderate to get the blurred version of the noisy image, whereas a 7×7 window is taken for high-noise. The Prewitt operator is then used on the resulted blurred image to find the edges. A small amount of noise still remains in different regions even after

passing the noisy image through the mean filter. The Prewitt operator is less sensitive to isolated high intensity point variations since the local averaging over sets of three pixels tends to reduce this. In effect, it is a 'small bar' detector, rather than a point detector. Secondly, it gives an estimate of edge direction as well as edge magnitude at a point which is more informative.

Fig (1): Blurred Image resulted from median filter

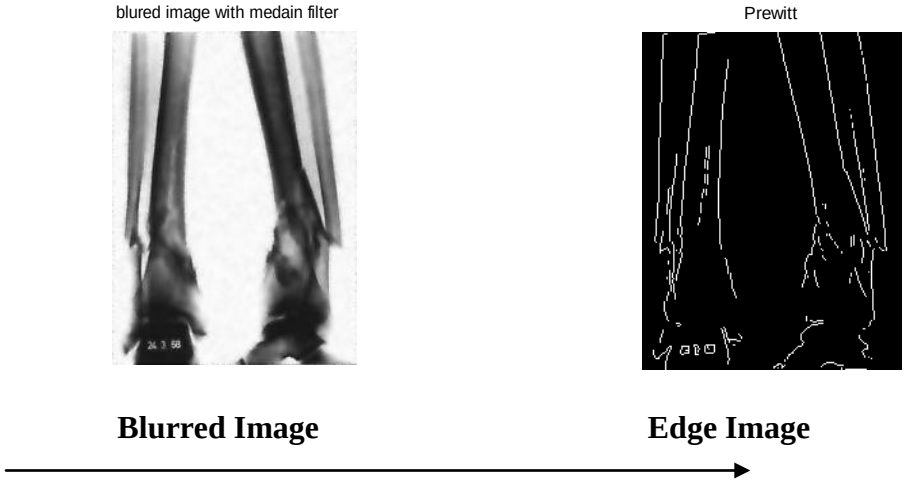

Fig (2) Edge Image using 'Prewitt' operator

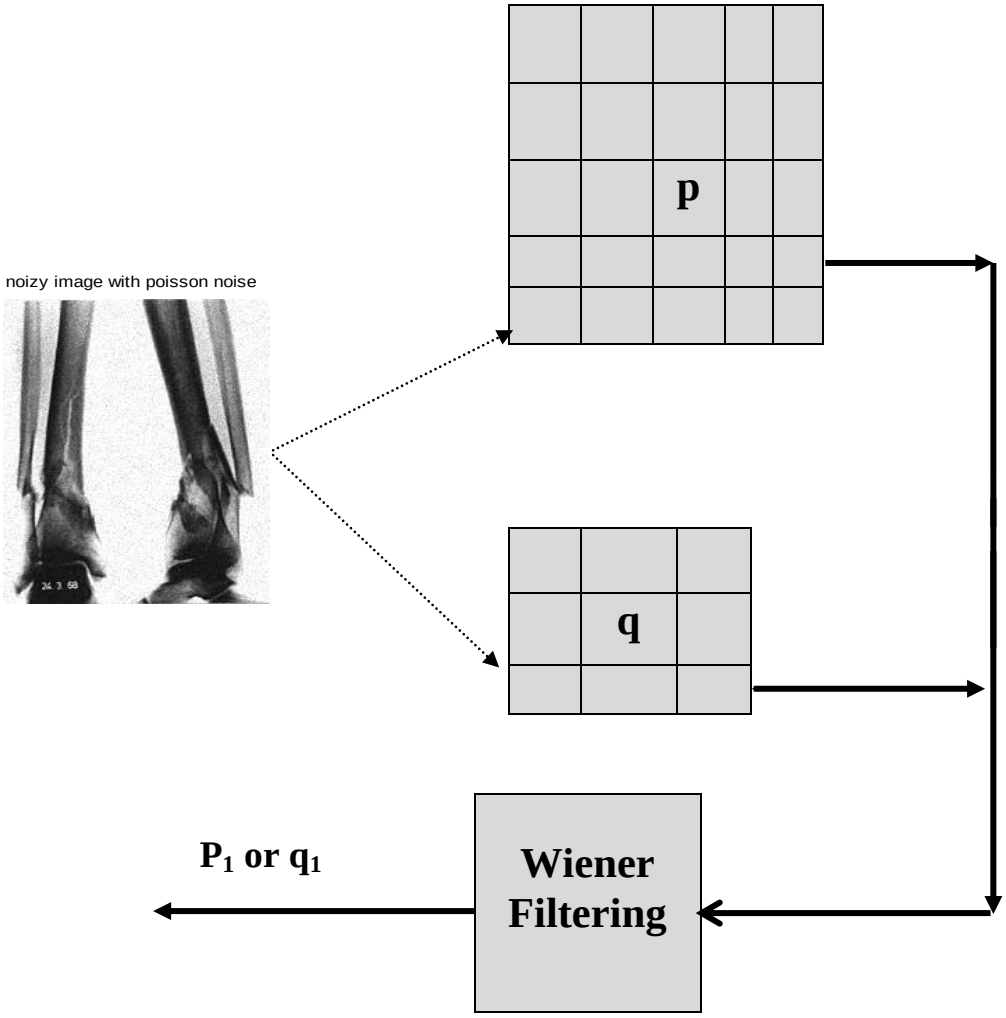

Fig (3) Filtering operation of AWWF for the pixels 'p' (belonging to smooth region) and 'q' (belonging to edge region)
The pixels 'p_1' and 'q_1' are the filtered pixels for the corresponding pixels 'p' and 'q' respectively.

7.1 The proposed Algorithm

The proposed algorithm is given below.

Step-1:

Read the original medical image (in this work used two types of medical image X-ray and MRI images),this images with variant size, and then add selective type of additive noises which are explained in this research of selected image to produced noisy image

Step-2:

The noisy image is passed through a median filter, as shown in Fig. (1), to get a blurred version of the image.

Step-2:

Edge operator (**Prewitt operator**) is applied on the blurred image, obtained in Step-2 to get the edge image. The pixels belong to smooth region and edge region are identified as ‘p’ and ‘q’, respectively. This operation is shown in Fig. (2).

Step-3:

Adaptive window Wiener filter is applied on the noisy image. The size of the window is varied with the following concepts.

- *If the center pixel is an **edge** pixel, then the size of the window is **small**;*
- *If the center pixel belongs to **smooth region**, the size of the window is **large**.*
- *If the noise power is **low** ($\sigma_n \leq 10$), then the size of the window is **small**;*
- *If the noise power is **moderate** ($10 < \sigma_n \leq 30$), then the size of the window is **medium**;*
- *If the noise power is **high** ($30 < \sigma_n \leq 50$), then the size of the window is **large**.*

This adaptive filtering concept is depicted in Fig. (3)

The noise power can be determined by using the value of the ($\sigma^2_{n)}$ Noise Variance of the noisy image.

Step-4:

All the filtered pixels are united together to obtain the denoised (filtered) image. The exact window sizes taken for various conditions are presented in the next sub-section.

7.2 Results and discussion

In this research the proposed algorithm has been applied on different medical images with variant sizes in a general N x M image and modalities affected by the appropriate noise and its performance was compared with other denoising methods.

The performance of the adaptive window wiener algorithm (AWWA) was compared with the other type of filters (wiener filter). The selection of window in this work is based on the level of noise present in the noisy image. If the noise level is unknown, a robust median estimator may be applied to predict the level of noise. When the noise level is ***low*** *($\sigma_n \leq 10$)* a 3×3 window is selected for filtering the noisy pixels belonging to homogenous regions; the pixel is unaltered if the noisy pixels belong to edges. When the noise level is ***moderate*** *($10 < \sigma_n \leq 30$),* a 5×5 window is chosen for filtration of noisy pixels of flat regions; the window size is 3×3 if the noisy pixels to be filtered are identified as edge pixels. When the noise level is ***high*** *($30 < \sigma_n \leq 50$),* a 7×7 window is used for filtration of noisy pixels of flat regions; if the noisy pixels are identified as edge pixels the window size used is 5×5.

In this work The Wiener filter was implemented using the adaptive filter, wiener2, in the MATLAB tool box function with a window of size 5 x 5 pixels. Fig. (4) Illustrates the visual comparison between the proposed algorithm and the other methods that were applied for denoising "X-Ray" image corrupted by Poisson noise. Fig. (5) Illustrates the visual comparison between the denoising methods applied on "MRI" image of corrupted by Rician noise.

The table(1) and (2) explain the PSNR and Root-Mean-Squared Error (RMSE) values of experiment results of adaptive window wiener algorithm and show comparison in performance with standard filters (median and wiener) filters of two type of medical images with two test images x-ray image and MRI( ) image.

Extensive computer simulation is carry out on MATLAB 9 platform to access the performance of the proposed filters (Adaptive Window Wiener Filter (AWWF)), and standard existing filters (Median filter, Wiener filter). The test images are X-ray image of size (129 x 250) dimension corrupted with Poisson noise, and the second type of medical image is MRI of size (207 x 256) dimension corrupted with Rician noise. The standard deviation σ_2 = 5, 10, 15, 20, 25, and 30 are used for testing the filtering performance: The peak signal to noise ratio (PSNR), root mean square error (RMSE), method noise and execution time are taken as performance measures.

Table-1: Filtering performance of various filters, in terms of PSNR (dB), operated on x-ray image under various noise conditions (σ_n varies from 5 to 30).

Peak-Signal-to-Noise Ratio, PSNR (dB)							
Denoising Filters	**Standard deviation of Poisson noise**						**Execution time (seconds)**
	5	**10**	**15**	**20**	**25**	**30**	
Test Image: X-ray							
Median [3×3]	33.51	30.57	30.10	28.13	26.48	25.10	4.12
Median [5×5]	32.20	29.76	31.30	29.96	28.72	27.64	4.75
Median [7×7]	31.19	28.62	30.75	29.87	29.00	28.23	5.62
Wiener [3 ×3]	36.83	32.51	31.07	29.34	27.28	25.81	7.36
Wiener [5 ×5]	35.57	31.94	30.47	29.19	28.00	27.96	7.76
Wiener [7 ×7]	34.72	31.54	30.46	29.44	28.57	27.78	8.12
AWWA	37.18	35.36	33.78	32.56	31.29	30.13	9.28
	Standard deviation of Rician noise						**Execution time (seconds)**
	5	**10**	**15**	**20**	**25**	**30**	
Test Image: MRI							
Median [3×3]	34.55	32.57	30.10	28.13	26.48	25.22	4.18
Median [5×5]	33.23	32.76	31.30	29.96	28.72	27.61	5.13
Median [7×7]	32.19	31.62	30.75	29.87	29.00	28.27	6.15
Wiener [3 ×3]	38.11	34.45	31.77	29.44	27.56	25.49	8.23
Wiener [5 ×5]	37.67	33.82	32.16	30.74	29.41	28.18	8.91
Wiener [7 ×7]	35.98	32.52	31.25	30.08	29.06	28.15	9.60
AWWA	37.16	35.91	33.68	32.01	31.14	30.21	11.22

Table-2: Filtering performance of various filters, in terms of RMSE, operated on a Lena image under various noise conditions (σ_n varies from 5 to 30).

Root-Mean-Squared Error (RMSE)						
Denoising Filters	**Standard deviation of Poisson noise**					
	5	**10**	**15**	**20**	**25**	**30**
Test Image: X-ray						
Median [3×3]	4.24	6.27	8.18	10.20	12.24	14.35
Median [5×5]	6.34	7.395	8.26	9.30	10.35	11.57
Median [7×7]	8.23	8.84	9.40	9.99	10.63	11.39
Wiener [3 ×3]	3.11	5.07	6.88	8.87	10.88	12.90
Wiener [5 ×5]	3.82	5.73	6.78	7.87	9.02	10.17
Wiener [7 ×7]	4.22	6.73	7.62	8.59	9.48	10.40
AWWA	4.50	5.12	5.85	7.23	7.89	9.53
	Standard deviation of Rician noise					
	5	**10**	**15**	**20**	**25**	**30**
	Test Image: MRI					
Median [3×3]	4.11	6.22	8.18	10.20	12.24	14.35
Median [5×5]	6.28	7.31	8.26	9.30	10.35	11.57
Median [7×7]	8.31	8.88	9.40	9.99	10.63	11.39
Wiener [3 ×3]	3.40	5.27	6.88	8.87	10.88	12.90
Wiener [5 ×5]	3.91	5.73	6.78	7.37	9.12	10.34
Wiener [7 ×7]	4.32	6.83	7.62	8.59	9.48	10.44
AWWA	4.61	5.32	5.91	6.12	7.19	8.23

(a) Original Image (129 x 250)

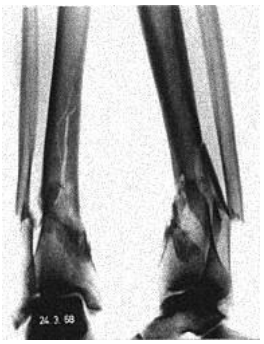

(b) Noisy Image (Poisson)

(c) Wiener Filter (5 x 5 pixel)

(d) The Proposed Algorithm

Fig (4): Denoising of "X-Ray" image. (a) original image (b) noisy Image with Poisson noise (c) denoised image using Wiener Filter (d) denoised image using the proposed algorithm implemented with median filter coefficients and window size 5×5.

(a) Original Image (256 x 207)

(b) Noisy Image (Rician)

(c) Wiener Filter (5 x 5 pixel)

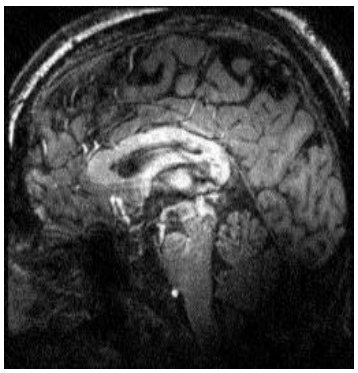

(d) The Proposed Algorithm

Fig (5): Denoising of "MRI" image , (a) original image, (b) noisy image, (c) denoised image using Wiener Filter, (d) denoised image using the proposed algorithm implemented with window size 7×7.

Figure (6) shows the original image with noisy image and denoising image in the same windows implemented by using matlab application with version 2009 and display the values of mean square errors (MSE), in addition to signal to noise ratio for each original image and denoising image, also determined the value of PSNR and execution time with run date.

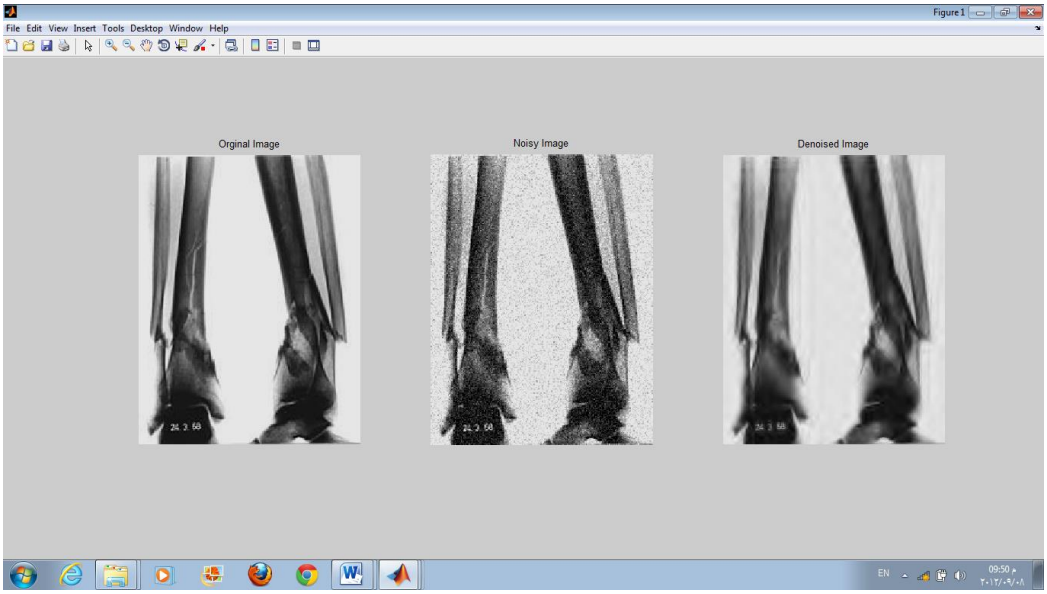

MSE is 1.856795 * 10^3
SNRo is 24.924491 dB.
SNRi is 25.201358 dB.
PSNR is 27.312360 dB.
Execution Time is 0.951606 seconds.
Current Date is 08-Sep-2012

Fig (6): Denoising of "x-ray" image using the proposed algorithm implemented withwindow size 7×7.

7.3 Conclusions

It is observed that the proposed filter: AWWF is very efficient in suppressing Poisson and Riacin from images. It is seen that AWWF outperforms the other existing spatial-domain filters in suppressing additive noise under moderate noise ($10 < \sigma_n \leq 30$) conditions. The PSNR values are relatively high as compared to other filters under moderate noise conditions. Hence, it may be concluded that the AWWF is best spatial-domain filter in suppressing additive noise under moderate noise conditions. It preserves the edges and fine details very well, as observed in Fig.(4)compared to other filters. The filter does not perform well under high noise conditions as observed in Fig. (4), and (5) and tables (1, 2).

The execution time, taken by a filter is an important measure to find its computational complexity. It is observed from table-2 that the proposed filter AWWF is observed to possess moderate computational complexity. The filter retains the detailed information very well as compared to other spatial-domain filters. Thus, the proposed filtering scheme is observed to be very good spatial domain image denoising filters.

According to the experiment results in Table-1and Table-2 the values of PSNR decreasing when the values of standard deviation ($\sigma_{2)}$ increasing. Otherwise the values of RMSE increasing when the values of standard deviation ($\sigma_{2)}$ decreasing.

Reference

Abdulmunim, M.E. **'Color Image Denoising Using Discrete Multiwavelet Transform'**, Ph.D. Thesis, University of Technology, Department of Computer Science, May 2004.

Achim, A.; A. Bezerianos, and P. Tsakalides, **'Novel Bayesian Multiscale Method for Speckle Removal in Medical Ultrasound Images'**, IEEE Transactions on Medical Imaging, Vol. 20, No. 8, pp. 772-783, August 2001.

Angenent, S. ; E. Pichon, and A. Tannenbaum, **'Mathematical Methods in Medical Image Processing'**, Bulletin, (New Series) of the American Mathematical Society, Volume 43, Number 3, pp. 365- 396, July 2006.

Buades, A.; B. Coll, and J. Morel, **'A non-local algorithm for image denoising'**, Proc. IEEE international conference on computer vision and pattern recognition, pp. 60-65, 2005.

Chaira, T. and A.K. Ray, **'A new measure using intuitionist fuzzy set theory and Its application to edge detection'**, Applied Soft Computing, vol. 8, no. 2, pp. 919-927, 2008.

Chang, S.; B. Yu, and M. Vetterli, **'Adaptive wavelet thresholding for image denoising and compression'**, IEEE Transactions on Image Processing, vol. 9, no. 9, pp. 1532-1546, 2000.

Dougherty, G. **'Digital Image Processing for Medical Applications'**, Cambridge University Press Cambridge, UK, 2009.

Gonzalez, R.C. and R. E. Woods, **'Digital Image Processing'**, Prentice Hall Inc., 2002.

Gravel, P.; G. Beaudoin, and J. A. De Guise, **'A Method for Modeling Noise in Medical Images'**, IEEE Transactions On Medical Imaging, Vol. 23, No. 10, pp. 1221-1232, October 2004.

Jang I. H. and N. C. Kim, **'Locally adaptive Wiener filtering in wavelet domain for image restoration'**, Proc. IEEE R-10 Conference on Speech and Image Technologies for Computing and Telecommunications, TENCON-97, vol. 1, pp. 25-28, 1997.

Rashid Ismael, M. **'MEDICAL IMAGE DENOISING BASED ON THE DUAL TREE COMPLEX DISCRETE WAVELET TRANSFORM'**, Submitted to the Department of Electrical and Electronic Engineering at the University of Technology, August 2011 A.D

Rodrigo R. and S. Pedrini, **' Adaptive Edge-Preserving Image Denoising Using Wavelet Transforms'**, Institute of Computing, University of Campinas, Campinas- SP, Brazil, 2012

Roy, S.; N. Sinha and A. K. Sen,**'A NEW HYBRID IMAG DENOISING METHOD',** International Journal of Information Technology and Knowledge Management July-December 2010, Volume 2, No. 2, pp. 491-497

Satheesh1, S. and K. Prasad, **' MEDICAL IMAGE DENOISING USING ADAPTIVE THRESHOLD BASED ON CONTOURLET TRANSFORM',** An International Journal (ACIJ), Vol.2, No.2, March 2011

Zhang, L.; W. Dong, D. Zhang, and G. Shi,**' Two-stage image denoising by principal component analysis with local pixel grouping'**, paper IEEE, 2009 Elsevier Ltd. All rights reserved.

Zhang, Y.; M. Brady, and S. Smith**, 'Segmentation of Brain MR Images through a Hidden Markov Random Field Model and the Expectation-Maximization Algorithm'**, IEEE Transactions on Medical Imaging, Vol. 20, No. 1, pp. 45-57, January 2001.